を用いて創製した TNFα変異体 (mTNF-K90R) が、①
in vitroにおける比活性が野生型 TNFα (wTNFα) の
数倍にも向上しつつ、プロテアーゼ抵抗性を有する
こと、②mTNF-K90R を抗原と共に経鼻投与すること
で、粘膜面・全身面で wTNFαよりも強い抗原特異的
免疫反応を誘導可能であることを示してきた。そこ
で本研究では、インフルエンザウイルスに対する効
果的な粘膜ワクチン開発を目標に、mTNF-K90R のイ
ンフルエンザウイルス抗原に対する粘膜免疫誘導能
を評価した。

　一方で近年、抗原遺伝子や免疫活性化遺伝子をア
デノウイルスベクター (Adv) で発現させるワクチン
法が高いワクチン効果を示すことから注目されてい
る。しかし、血球系細胞、樹状細胞などの免疫細胞
では、Adv のレセプターである CAR の発現が乏しい
ことから、十分な遺伝子導入を行えない結果、免疫
活性化能が不十分であるという問題点を抱えている。
従って、経粘膜投与可能で、かつ十分な遺伝子導入
効率を誇る Adv の開発が、将来的な粘膜ワクチンへ
の適用に必要不可欠と考えられる。本観点から我々
は、細胞内移行活性を有する Tat ペプチドや R8 ペプ
チドを Adv 表面に化学結合させることによって、CAR
の発現していない細胞に対しても効率良く遺伝子導
入可能であることを示してきた。そこで本研究では、
Tat 修飾 Adv (Tat-Adv) 及び R8 修飾 Adv (R8-Adv)
の各種細胞に対する遺伝子導入効率とともに、遺伝
子導入メカニズムに関して検討した。

B. 研究方法
・免疫方法；BALB/c マウス (6〜8 週齢、雌性) への
経鼻免疫は、サイトカインあるいはコレラトキシン
B サブユニット (CT-B ; List Biological
Laboratories)をインフルエンザウイルス抗原 HA
(Protein science、1 μg/mouse) と混合投与し、
非麻酔条件下で行なった。尚、投与スケジュールは
4 週間間隔で 2 回行った。

・サンプルの回収方法；最終免疫から 2 週間後に眼底
採血を行い、11000 rpm、 10 分遠心操作を行うこと

により血清を回収した。

・OVA 特異的抗体産生能の評価 (HA specific Ig
ELISA)；HA (2 μg/mL、in 50 mM Bicarbonate Buffer)
を ELISA プレートに加え、4 ℃ で一晩放置すること
で固相した。PBS で 2 倍希釈した Block Ace でブロ
ッキング (室温、1 時間) した後、各濃度に調製し
たサンプルを加えてインキュベートした (室温、2
時間；IgG、37 ℃、2 時間；IgA)。これらのプレー
トを 0.05 % Tween 含有 PBS (PBST) あるいは、
0.05 % Tween 含有 TBS (TTBS) で洗浄後、各濃度
に調製した HRP 標識 IgG 抗体およびビオチン標識
IgA 抗体 (Southern Biotech) を加えてインキュベ
ートした (室温、2 時間；IgG、37 ℃、2 時間；IgA)。
プレートを洗浄した後、1/2500 に希釈した HRP 標識
ストレプトアビジン (ZyMed) を加え、さらに室温で
1 時間反応させた。再度、洗浄操作を行い最後に蒸
留水で洗浄した後、TMBZ 基質液を添加した。2N H_2SO_4
を添加することにより発色反応を停止させ、吸光波
長 450 nm、副波長 690 nm における吸光度を測定し
た。尚、抗体価は非免疫マウスよりも吸光度が 0.1
以上高い最大希釈倍率を Reciprocal Log2 Titer で
表した。

ベクターの作製、精製、および力価測定；Advは、
水口らが開発した改良 in vitro ligation法に準拠し
て作製した。本研究では、Cytomegalovirusプロモー
ター制御下にホタルルシフェラーゼを発現するAdv
を構築した。作製した各種Advは、293 細胞を用いて
増幅し、塩化セシウム密度勾配遠心法にて精製した。
また、Adv粒子数 (vector particle; VP) の測定は
Maizelらの方法に準拠した。

活性基を有するTatペプチド、R8 ペプチドの合成と
Tat-Adv 、 R8-Adv の 作 製 ；Tat ペプチド
(GRKKRRQRRRPPQ)、R8 ペプチド (RRRRRRRR) に活性
基を付与したTat-NHS、R8-NHSを作製した。AdvのTat、
R8 ペプチド修飾は、Adv1 粒子あたりのカプシドタン
パクに存在するリジン残基に対して 25 倍モル量に
相当するTat-NHS、R8-NHSをAdv懸濁液 (final 2 ×

10^{11} VP/ml）と混合し、300 rpm で撹拌しながら 37°C で 45 分間反応させることにより行った。

Tat-Adv、R8-Adv の *in vitro* 遺伝子導入効率の評価；
未修飾 Adv、Tat-Adv あるいは R8-Adv を 300〜10000 VP/cell で用いて B16BL6 細胞、CT26 細胞、A549 細胞に遺伝子導入した。24 時間培養した後、これらの細胞における導入遺伝子（ルシフェラーゼ遺伝子）の発現を指標に遺伝子導入効率を評価した。

C. 研究結果

　本研究では、インフルエンザウイルスに対する効果的な粘膜ワクチン開発を目標に、医薬価値に優れたサイトカイン変異体を、安全性・有効性に優れた粘膜ワクチンアジュバントへ適用するための基礎検討を行った。本年度は、我々がこれまでに独自の技術で創製した TNFα 変異体である mTNF-K90R を用い、インフルエンザウイルス抗原に対する免疫誘導能を評価した。まず、mTNF-K90R を HA と共に経鼻免疫し、血清中の HA 特異的 IgG 誘導能を評価した（Figure 1）。その結果、mTNF-K90R は HA 単独投与群と比較して、有意な HA 特異的 IgG 産生の増加がみられ、ポジティブコントロールとしての CT-B に匹敵する抗体産生能を有していた。次に、粘膜面における免疫誘導を、鼻粘膜組織および唾液中における、HA 特異的 IgA 産生を指標に検討した（Figure 2, 3）。その結果、mTNF-K90R は HA 単独投与群と比較して、HA 特異的 IgA 産生が有意に向上しており、CT-B と同等あるいはそれ以上の活性を有している可能性が示唆された。以上の結果から、mTNF-K90R はインフルエンザウイルスに対する有効な粘膜ワクチンアジュバントになり得る可能性が示唆された。

　次に、将来的な粘膜ワクチンへの応用を念頭に、遺伝子導入効率に優れた Adv の創製を試みるとともに、その遺伝子導入メカニズムに関して検討した。まず、Adv 表面のペプチド結合部位（リジン残基）に対して 25 倍モル量の活性基付与型 Tat ペプチド、R8 ペプチドを混合することによって、ルシフェラーゼ遺伝子を発現する Tat-Adv、R8-Adv を作製した。

これら Adv を用いて B16BL6 細胞、CT26 細胞、A549 細胞に遺伝子導入し、24 時間培養後のルシフェラーゼ発現レベルを指標に各ベクターの遺伝子導入活性を比較した（Figure 4）。その結果、CAR 低発現の B16BL6 細胞、CT26 細胞において、Tat-Adv、R8-Adv は未修飾 Adv と比較して 10-100 倍高い遺伝子導入を達成した。また、CAR 高発現の A549 細胞においては、Tat-Adv 及び R8-Adv は未修飾 Adv とほぼ同等の遺伝子発現活性を示した。

　次に、Tat-Adv 及び R8-Adv の高い遺伝子導入効率に関して、そのメカニズムを検討した。一般に、Tat ペプチドや R8 ペプチドは、細胞表面のヘパラン硫酸などの負電荷を有する糖鎖に結合し、その後エンドサイトーシスの一種であるマクロピノサイトーシスにより効率的に細胞内に取り込まれることが知られている。そこでまず、Tat-Adv 及び R8-Adv の遺伝子導入におけるマクロピノサイトーシスの関与を検討した。マクロピノサイトーシス阻害剤であるアミロライド存在下での遺伝子導入を検討した結果、未修飾 Adv では全く遺伝子導入の低下が観察されないのに対し、Tat-Adv 及び R8-Adv では有意な遺伝子導入効率の低下が認められた（Figure 5）。以上の結果から、Tat-Adv 及び R8-Adv は、マクロピノサイトーシス依存的に細胞内に取り込まれることが示唆された。次に、ヘパラン硫酸と類似した構造を有するヘパリンと Adv を同時に作用されることで、遺伝子導入におけるヘパラン硫酸の関与について検討した。その結果、未修飾 Adv、R8-Adv では、ヘパリン共存下でも遺伝子導入効率が保持されたのに対して、Tat-Adv ではヘパリン濃度依存的に遺伝子導入効率の低下が観察された（Figure 6）。すなわち、Tat-Adv と R8-Adv では、細胞表面への接着において異なるメカニズムを有することが示された。そこで、同様の方法を用いて、コンドロイチン硫酸 A、コンドロイチン硫酸 B、コンドロイチン硫酸 C の関与を検討した。その結果、コンドロイチン硫酸 A、コンドロイチン硫酸 C では、未修飾 Adv、Tat-Adv、R8-Adv いずれも顕著な変化がみとめられないものの、コンドロイチン硫酸 B 共存下において、Tat-Adv、R8-Adv で遺伝子導入効率の低下が認められた（Figure 7）。以上の結果より、

R8-Adv の遺伝子導入メカニズムは未だ不明瞭なものの、Tat-Adv とは異なるメカニズムを有することが示された。

D. 考　察

　我々はこれまでに、TNF α 変異体である mTNF-K90R を粘膜ワクチンとして応用し、mTNF-K90R が有効な粘膜ワクチンアジュバントとして利用できる可能性を示してきた。しかし一般に、用いる抗原の抗原性によりその免疫誘導特性は変化することが知られている。本研究で、mTNF-K90R がインフルエンザウイルス抗原に対しても、効率良く免疫誘導を示したことから、mTNF-K90R が感染症ワクチンとしても有望であることが示された。すでに、mTNF-K90R の経鼻投与において、鼻腔で顕著な副作用を誘発しないことは確認しており、今後霊長類などを用いた有効性評価を進める予定である。また、mTNF-K90R により誘導された抗体が、インフルエンザウイルスの感染に対して中和能を保有しているかに関しても詳細な検討が必要と考えられる。

　近年、ワクチン素材として期待される Adv について、その感染域拡大を目指した結果、従来型 Adv では困難であった細胞にも効率的に遺伝子導入可能な Adv の創製に成功した。今後は、樹状細胞に対する遺伝子導入効率を検討するとともに、in vivo における粘膜免疫誘導能に関しても検討する必要がある。

E. 結論

　本研究では、我々が開発してきた TNFα 変異体 mTNF-K90R が、インフルエンザウイルスに対する粘膜ワクチンアジュバントになり得ることを示した。更に、あらゆる細胞に遺伝子導入可能な Adv の創製に成功し、その遺伝子導入メカニズムを明らかとした。

F. 健康危険情報

該当事項無し

G. 研究発表

①論文発表

1. Yoshioka Y, Asavatanabodee R, Eto Y, Watanabe H, Morishige T, Yao X, Kida S, Maeda M, Mukai Y, Mizuguchi H, Kawasaki K, Okada N, Nakagawa S. Tat conjugation of adenovirus vector broadens tropism and enhances transduction efficiency. Life Sci. 2008 Nov 21;83(21-22):747-55.

②学会発表

国内

1. 萱室裕之, 吉岡靖雄, 形山和史, 鎌田春彦, 野村鉄也, 阿部康弘, 廣井隆親, 角田慎一, 堤　康央：TNF スーパーファミリーに着目した粘膜ワクチンアジュバント能の体系的評価., 第 56 回 日本ウイルス学会学術集会, 岡山, 2008 年 10 月.

2. 鎌田春彦, 萱室裕之, 吉岡靖雄, 形山和史, 廣井隆親, 阿部康弘, 角田慎一, 堤　康央：活性増強型 TNF ・構造変異体の粘膜ワクチンアジュバントへの応用., 第 22 回 日本エイズ学会学術集会, 大阪, 2008 年 11 月.

3. 萱室裕之, 吉岡靖雄, 阿部康弘, 形山和史, 鎌田春彦, 野村鉄也, 廣井隆親, 角田慎一, 堤康央：活性増強型 TNF 変異体の粘膜ワクチンアジュバントへの応用., ファーマバイオフォーラム 2008, 東京, 2008 年 11 月.

4. 萱室裕之, 吉岡靖雄, 形山和史, 鎌田春彦, 野村鉄也, 阿部康弘, 廣井隆親, 角田慎一, 堤　康央：A bioactive mutant TNF (mTNF-K90R) elicited mucosal and systemic immunity against HIV-1 gp120 and influenza virus hemagglutinin., 第 38 回 日本免疫学会・学術集会, 京都, 2008 年 12 月.

5. 吉岡靖雄, 萱室裕之, 形山和史, 鎌田春彦, 野村鉄也, 阿部康弘, 廣井隆親, 角田慎一, 堤　康央：Identification of new candidates as mucosal vaccine adjuvant in TNF superfamily cytokines., 第 38 回 日本免疫学

会・学術集会，京都，2008 年 12 月.

6. 萱室裕之，吉岡靖雄，阿部康弘，形山和史，廣井隆親，角田慎一，堤　康央 : 活性増強型 TNF 変異体の粘膜ワクチンアジュバントへの応用.，日本薬学会　第 129 年回，京都，2009 年 3 月.

海外

1. Yoshioka Y, Asavatanabodee R, Eto Y, Watanabe H, Morishige T, Yao X, Kida S, Maeda M, Mukai Y, Mizuguchi H, Kawasaki K, Okada N, Nakagawa.Tat conjugation of adenovirus vector broadens tropism and enhances transduction efficiency. ASGT 11th Annual Meeting. May, 2008. Bosotn.

2. Yoshioka Y, Shinsaku Nakagawa. Tat conjugation of adenovirus vector broadens tropism and enhances transduction efficiency. 6th Symposium on Membrane Stress Biotechnology. September, 2008. Osaka.

3. Kayamuro H, Yoshioka Y, Katayama K, Kamada H, Nomura T, Abe Y, Hiroi T, Tsunoda S, Tsutsumi Y. MUTANT TNF ELICITS TH2-TYPE RESPONSES FOR ENHANCED MUCOSAL IMMUNITY. 7th Joint Conference of the Intenational Society for Interderon and Cytokine Research and International Cytokine Society., October, 2008. Montréal/Québec (CANADA).

4. Yoshioka Y, Kayamuro H, Katayama K, Kamada H, Abe Y, Hiroi T, Tsunoda S, Tsutsumi Y. IDENTIFICATION OF NEW CANDIDATES AS MUCOSAL VACCINE ADJUVANT IN TNF SUPERFAMILY CYTOKINES. FIMSA 2008, October, 2008. Taipei (Taiwan).

H. 知的財産権の出願・登録状況
①特許取得
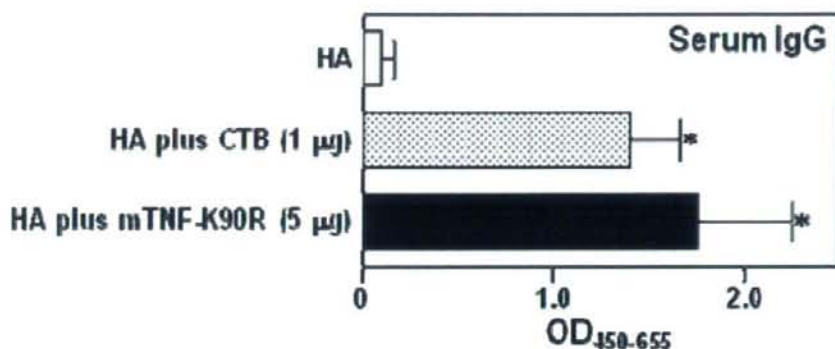該当事項無し

②実用新案登録
該当事項無し

③その他
該当事項無し

Figure 1. mTNF-K90R induced serum IgG responses against influenza virus HA in mice. BALB/c mice were immunized intranasally with HA together with 1 µg CTB or 5 µg mTNF-K90R. One week after the last immunization, the levels of HA-specific IgG in serum at a 1:500 dilution was assessed by ELISA at a 1:8 dilution. Data represents the mean of absorbance 450 nm (reference wavelength, 655 nm). Data are presented as means ± SEM (n = 4-6; * P < 0.05 *versus* value for HA alone treated group by ANOVA).
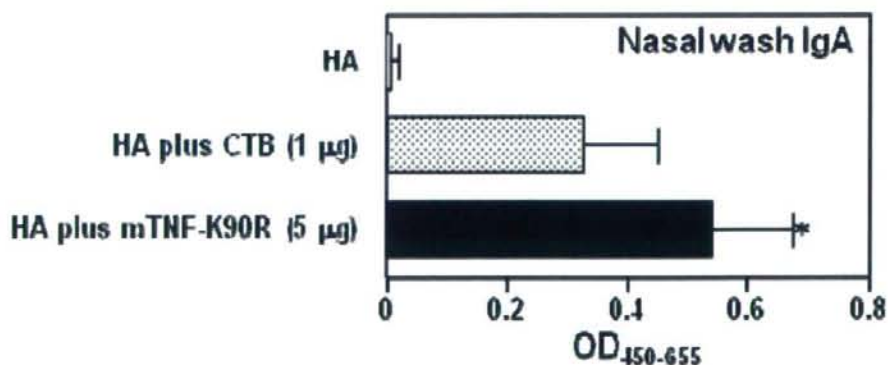

Figure 2. mTNF-K90R induced nasal IgA against influenza virus HA in mice. BALB/c mice were immunized intranasally with HA together with 1 µg CTB or 5 µg mTNF-K90R. One week after the last immunization, the levels of HA-specific IgA in nasal at a 1:8 dilution were assessed by ELISA at a 1:8 dilution. Data represents the mean of absorbance 450 nm (reference wavelength, 655 nm). N.D; not detected. Data are presented as means ± SEM (n = 4-6; * P < 0.05 *versus* value for HA alone treated group by ANOVA).
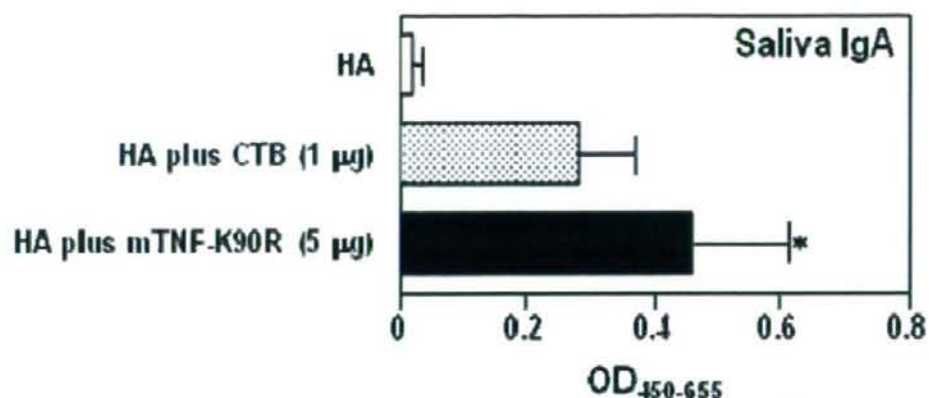
Figure 3. mTNF-K90R induced saliva IgA against influenza virus HA in mice. BALB/c mice were immunized intranasally with HA together with 1 μg CTB or 5 μg mTNF-K90R. One week after the last immunization, the levels of HA-specific IgA in saliva at a 1:8 dilution were assessed by ELISA at a 1:8 dilution. Data represents the mean of absorbance 450 nm (reference wavelength, 655 nm). N.D; not detected. Data are presented as means ± SEM (n = 4-6; * $P < 0.05$ *versus* value for HA alone treated group by ANOVA).
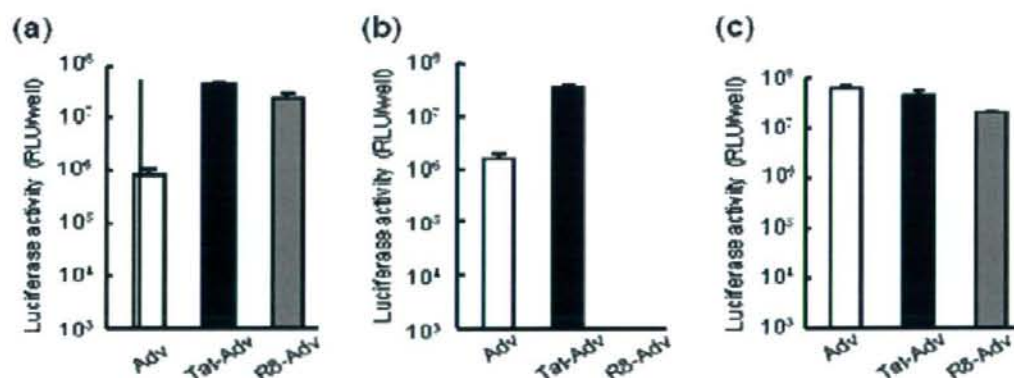

Figure 4. Transduction efficiency of CPP-Advs with various modification ratios into (a) B16BL6, (b) CT26, and (c) A549 cells. Cells (1 × 10⁴) were transduced with 1 × 10⁴ vp/cell of Tat-Adv, Pro-Adv, or R8-Adv encoding the luciferase gene. After 24 h of cultivation, luciferase expression was measured. Each bar represents the mean ± S.D. (n = 4). Each CPP-Adv was used at molar ratios of 1:25 (Adv lysine residue: CPP-NHS).
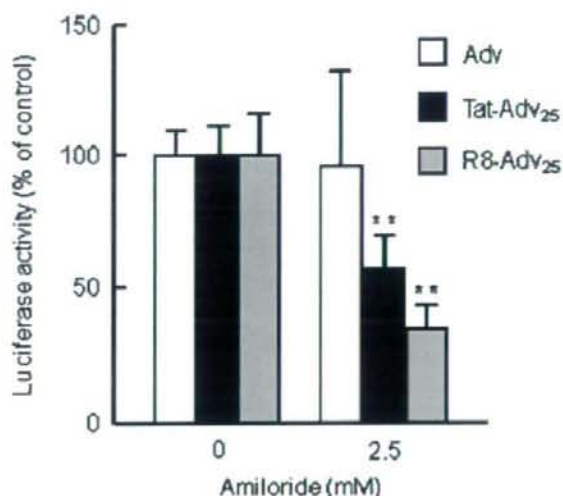
Figure 5. The cellular uptake of Tat-Adv and R8-Adv depends on macropinocytosis. A549 cells (1 × 10^4 cells) were transduced with 1 × 10^4 vp/cell for each vector in the absence or presence of 2.5 mM amiloride. After 24 h of cultivation, luciferase expression was measured. Each bar represents the mean ± S.D. (n = 5; ** $P < 0.01$ versus value for the absence of amiloride by Student's t-test)
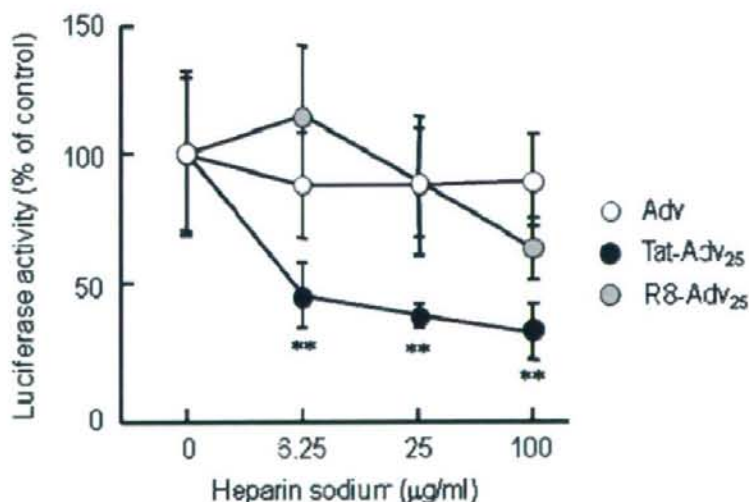

Figure 6. The cellular uptake of Tat-Adv and R8-Adv depends on heparan sulfate proteoglycans. A549 cells (1 × 10^4 cells) were transduced with 1 × 10^4 vp/cell of each vector in the absence or presence of 6.25, 25, or 100 µg/ml of heparin sodium. After 24 h of cultivation, luciferase expression was measured. Each bar represents the mean ± S.D. (n = 5; ** $P < 0.01$ versus value for absence of heparin sodium by ANOVA)
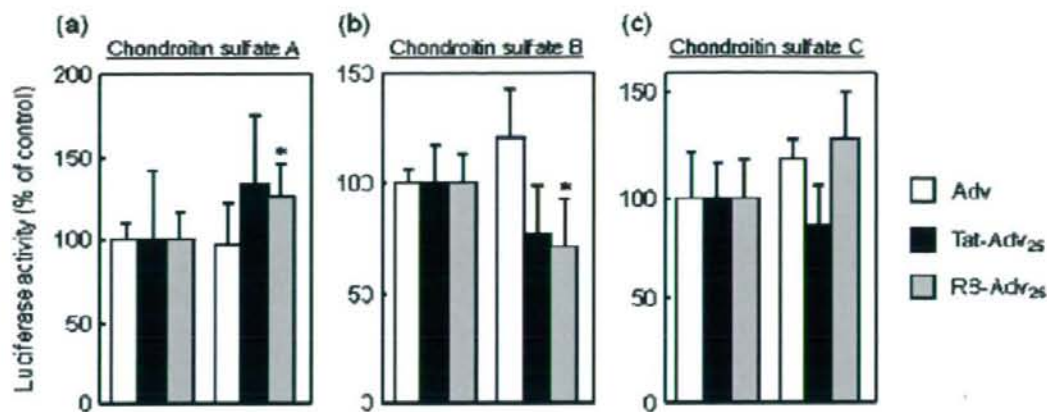
Figure 7. Cellular uptake of Tat-Adv and R8-Adv depends on chondroitin sulfate. A549 cells (1×10^4) were transduced with 1×10^4 vp/cell of each vector in the absence or presence of 90 µg/ml of (a) chondroitin sulfate-A, (b) chondroitin sulfate-B, or (c) chondroitin sulfate-C. After 2 h incubation, the cells were washed twice by PBS, and the virus solution was replaced with fresh medium. After 24 h cultivation, luciferase expression was measured. Each point represents the mean ± S.D. (n = 5; * $P <$ 0.05 versus value for the absence of chondroitin sulfate by Student's t-test)

研究成果の刊行に関する一覧表

書籍

著者氏名	論文タイトル名	書籍全体の編集者名	書 籍 名	出版社名	出版地	出版年	ページ
該当なし							

雑誌

発表者氏名	論文タイトル名	発表誌名	巻号	ページ	出版年
Shibata H., Yoshioka Y., Ohkawa A., Abe Y., Nomura T., Mukai Y., Nakagawa S., Taniai M., Ohta T., Mayumi T., Kamada H., Tsunoda S., Tsutsumi Y.	The therapeutic effect of TNFR1-selective antagonistic mutant TNF-alpha in murine hepatitis models.	Cytokine	44	229-233	2008
Abe Y., Yoshikawa T., Kamada H., Shibata H., Nomura T., Minowa K., Kayamuro H., Katayama K., Miyoshi H., Mukai Y., Yoshioka Y., Nakagawa S., Tsunoda S., Tsutsumi Y.	Simple and highly sensitive assay system for TNFR2-mediated soluble- and transmembrane-TNF activity.	J. Immunol. Methods.	335	71-78	2008
Yoshioka Y., Asavatanabodee R., Eto Y., Watanabe H., Morishige T., Yao X., Kida S., Maeda M., Mukai Y., Mizuguchi H., Kawasaki K., Okada N., Nakagawa S.	Tat conjugation of adenovirus vector broadens tropism and enhances transduction efficiency.	Life Sci.	83	747-755	2008
Mukai Y., Shibata H., Nakamura T., Yoshioka Y., Abe Y., Nomura T., Taniai M., Ohta T., Ikemizu S., Nakagawa S., Tsunoda S., Kamada H., Yamagata Y., Tsutsumi Y.	Structure-function relationship of tumor necrosis factor (TNF) and its receptor interaction based on 3D structural analysis of a fully active TNFR1-selective TNF mutant.	J. Mol. Biol.	385	1221-1229	2009
Mukai Y., Nakamura T., Yoshioka Y., Shibata H., Abe Y., Nomura T., Taniai M., Ohta T., Nakagawa S., Tsunoda S., Kamada H., Yamagata Y., Tsutsumi Y.	Fast binding kinetics and conserved 3D structure underlie the antagonistic activity of mutant TNF: useful information for designing artificial proteo-antagonists. J. Biochem.				in press

CYTOKINE

ELSEVIER

The therapeutic effect of TNFR1-selective antagonistic mutant TNF-α in murine hepatitis models

Hiroko Shibata [a,b], Yasuo Yoshioka [a,c,d], Akiko Ohkawa [a,d], Yasuhiro Abe [a,d], Tetsuya Nomura [a,d], Yohei Mukai [a,d], Shinsaku Nakagawa [d], Madoka Taniai [e], Tsunetaka Ohta [e], Tadanori Mayumi [f], Haruhiko Kamada [a,c], Shin-ichi Tsunoda [a,c,*], Yasuo Tsutsumi [a,c,d]

[a] Laboratory of Pharmaceutical Proteomics, National Institute of Biomedical Innovation (NIBIO), 7-6-8 Saito-Asagi, Ibaraki, Osaka 567-0085, Japan
[b] National Institute of Health Science, Kamiyoga 1-18-1, Setagaya-ku, Tokyo 158-8501, Japan
[c] The Center for Advanced Medical Engineering and Informatics, Osaka University, 1-6 Yamadaoka, Suita, Osaka 565-0871, Japan
[d] Graduate School of Pharmaceutical Sciences, Osaka University, 1-6 Yamadaoka, Suita, Osaka 565-0871, Japan
[e] Biomedical Institute, Research Center, Hayashibara Biochemical Laboratories, Inc., 675-1 Fujisaki, Okayama 702-8006, Japan
[f] Faculty of Pharmaceutical Sciences, Kobe Gakuin University, 518 Arise, Igawadani, Nishi-ku, Kobe 651-2180, Japan

ARTICLE INFO

ABSTRACT

Tumor necrosis factor-α (TNF-α) is critically involved in a wide variety of inflammatory pathologies, such as hepatitis, via the TNF receptor-1 (TNFR1). To develop TNFR1-targeted anti-inflammatory drugs, we have already succeeded in creating a TNFR1-selective antagonistic mutant TNF-α (R1antTNF) and shown that R1antTNF efficiently inhibits TNF-α/TNFR1-mediated biological activity in vitro. In this study, we examined the therapeutic effect of R1antTNF in acute hepatitis using two independent experimental models, induced by carbon tetrachloride (CCl_4) or concanavalin A (ConA). In a CCl_4-induced model, treatment with R1antTNF significantly inhibited elevation in the serum level of ALT (alanine aminotransferase), a marker for liver damage. In a ConA-induced T-cell-mediated hepatitis model, R1antTNF also inhibited the production of serum immune activated markers such as IL-2 and IL-6. These R1antTNF-mediated therapeutic effects were as good as or better than those obtained using conventional anti-TNF-α antibody therapy. Our results suggest that R1antTNF may be a clinically useful TNF-α antagonist in hepatitis.

© 2008 Elsevier Ltd. All rights reserved.

1. Introduction

Acute and chronic liver failure represents a worldwide health problem in humans for which there is no effective pharmacological treatment. For example, fulminant liver failure (FLF) is a devastating liver disease that is associated with significant mortality (40–80%) worldwide [1–3]. The incidence of FLF has increased in the last decade accounting for >2000 deaths annually in the United States alone [2]. Various etiologies result in acute and chronic liver failure. Immune-mediated mechanisms play a central role in autoimmune and viral hepatitis and thus determine disease progression.

Molecules belonging to the Tumor necrosis factor (TNF) superfamily, especially TNF-α, play an integral role in the regulation of innate and adaptive immunity, as well as contributing to inflammatory responses [4,5]. Overproduction of TNF-α has been implicated in the pathogenesis of various inflammatory conditions

including autoimmune diseases [4]. Recent studies suggest that TNF-α may also play a crucial role in the progression of liver failure [6–8]. Elevated levels of TNF-α occur in various acute and chronic liver diseases, including viral and alcoholic hepatitis, FLF, and exposure to hepatotoxins [9,10]. Thus, TNF-α appears to be involved in mediating hepatic cell death in experimental models of hepatitis. Furthermore, the inhibition of TNF-α by means of antibody (Ab) or soluble decoy receptors has proven to have a clinical benefit [11,12]. However, these therapies can cause serious side effects, such as bacterial and virus infection, lymphoma development, and lupus inflammatory disease, because they also inhibit the TNF-α-dependent host defense function of the patients [13,14]. TNF-α binds to two receptor-subtypes, p55 TNF receptor (TNFR1) and p75 TNF receptor (TNFR2), to exert its biological activities [15]. The two receptors have distinct biological functions with different distribution patterns; TNFR1 is constitutively expressed in most tissues, whereas expression of TNFR2 is highly regulated and is typically found in cells of the immune system [16]. It is generally believed that most of the TNF-α activities, including inflammatory responses in hepatitis, are triggered by TNFR1, whereas TNFR2 plays a pivotal role in regulating the immune response [15,17,18]. Unfortunately, the therapies with Ab or soluble decoy

* Corresponding author. Address: Laboratory of Pharmaceutical Proteomics, National Institute of Biomedical Innovation, 7-6-8 Saito-Asagi, Ibaraki, Osaka 567-0085, Japan. Fax: +81 72 641 9817.
E-mail address: tsunoda@nibio.go.jp (S. Tsunoda).

receptors affect the TNFR2-mediated activities of TNF-α, which are essential for immune function. Therefore, these therapies also have the potential to cause serious side effects, such as an increased risk of reactivating infectious disease or lymphoma. It is hoped that these problems can be overcome by the use of TNFR1-specific agents that selectively inhibit TNF-α-bioactivity through TNFR1 without interfering with TNFR2.

We have developed a novel technology to produce TNF-α muteins which bind to independent TNFRs using a unique phage-display method [19–21]. Recently we succeeded in producing a novel TNFR1-selective antagonistic mutant TNF-α (R1antTNF) using phage-display [21]. We showed that R1antTNF displays exclusive TNFR1 selective binding, which leads to effective and selective inhibitory effects of TNFR1-mediated biological activity both in vitro and in vivo without affecting TNFR2-mediated bioactivity [21].

In this study, we examined the therapeutic effect of R1antTNF in acute hepatitis using two independent experimental models, induced by carbon tetrachloride (CCl₄) or concanavalin A (ConA). R1antTNF showed anti-inflammatory effect on both acute hepatitis models. Especially, in CCl₄-induced acute hepatitis, R1antTNF showed superior therapeutic effect compared to the common anti-TNF-α Ab. These results indicate that R1antTNF can be a clinically useful TNF-α antagonist for the treatment of inflammatory diseases such as hepatitis.

2. Materials and methods

2.1. Cytokines and antibodies

Recombinant human wild-type TNF-α (wtTNF-α) and R1antTNF were purified as previously described [21]. Briefly, recombinant TNF-α s produced in *Escherichia coli* BL21(DE3) were recovered from inclusion bodies, washed in Triton X-100 and then solubilized in 6 M guanidine–HCl, 0.1 M Tris–HCl, pH 8.0 and 2 mM EDTA. Solubilized protein at 10 mg/ml was reduced with 10 mg/ml dithioerythritol for 4 h at room temperature and refolded by 100-fold dilution in a refolding buffer; 100 mM Tris–HCl, 2 mM EDTA, 0.5 M arginine and oxidized glutathione (551 mg/l). After dialysis against 20 mM Tris–HCl pH 7.4, containing 100 mM urea, active trimeric proteins were purified by Q-Sepharose (GE Healthcare Bioscience, Tokyo, Japan) and MonoQ chromatography (GE Healthcare Bioscience). Additionally, size-exclusion chromatography (Superose 12; GE Healthcare Bioscience) was performed. The endotoxin level of the purified TNF-αs were determined to be <300 pg/mg. Anti-mouse TNF-α Ab (MP6-XT3) was purchased from BD Biosciences Pharmingen (Franklin Lakes, NJ).

2.2. Cell culture

HEp-2 cells (a human laryngeal squamous cell carcinoma cell line) were provided by Cell Resource Center for Biomedical Research (Tohoku University, Sendai, Japan) and were maintained in RPMI 1640 (Sigma–Aldrich Japan, Tokyo, Japan) supplemented with 10% FBS and antibiotics. PC60-hTNFR1(+) cells (a mouse-rat fusion hybridoma consisting of human TNFR1-expressing PC60 cells) were generously provided by Dr. Vandenabeele (University of Gent, Belgium) [22], and maintained in RPMI 1640 supplemented with 10% FBS, 1 mM sodium pyruvate, 5×10^{-5} M 2-ME, 3 mg/ml puromycin (Wako Pure Chemical Industries, Osaka, Japan) and 1% antibiotic cocktail.

2.3. Cytotoxicity assay

For the inhibition assay, human HEp-2 cells were cultured in the 96-well plates (4×10^4 cells/well) in the presence of a constant

concentration of the human wtTNF-α (20 ng/ml) and a serial dilution of the R1antTNF with 100 μg/ml cycloheximide. After incubation for 18 h, cell survival was determined using the methylene blue assay as described previously [21].

2.4. PC60-hTNFR1(+) assay

PC60-hTNFR1(+) were cultured at 5×10^4 cells/well with IL-1β (2 ng/ml). To evaluate the inhibitory activity, serially diluted R1antTNF and human wtTNF-α (200 ng/ml) were added. After 24 h incubation, the amount of rat GM-CSF produced was quantified by ELISA according to the manufacturer's protocol (R&D Systems, Minneapolis, MN).

2.5. Mice

BALB/c mice (6-week-old females) were purchased from CLEA Japan (Tokyo, Japan). All experimental protocols for animal studies were in accordance with "*Principles of Laboratory Animal Care*" (National Institutes of Health publication no. 85-23, revised 1985) and our institutional guidelines.

2.6. Hepatitis model

In the CCl₄-induced hepatitis model, mice were injected intraperitoneally with CCl₄ at a dose of 0.1 ml/kg in corn oil (10 ml/kg). Control mice received only corn oil. In this model, serum TNF-α levels reached maximum levels 12 h after treatment with CCl₄. R1antTNF and anti-mouse TNF-α Ab were administered intravenously to each group at 12 h after CCl₄ administration. Blood samples were taken at 48 h after CCl₄ administration under light ether anesthesia. In the ConA-induced hepatitis model, mice were injected intravenously with ConA (0.4 mg/mouse). Anti-mouse TNF-α Ab or R1antTNF was injected intravenously at 1 h after administration of ConA. Blood samples were taken at 4 h after ConA administration under light ether anesthesia.

2.7. Measurement of serum ALT and cytokine concentrations

Serum ALT concentration was measured using a colorimetric test (Wako Pure Chemical Industries). Serum IL-2 and IL-6 were determined by sandwich ELISA kits (DuoSet ELISA Development Systems; R&D systems). Serum samples were accordingly diluted with 1% BSA in PBS and then applied to a capture antibody-coated immunoplate. All procedures were according to the manufacturer's protocol. The ELISA detection limit was 10 pg/ml.

2.8. Statistical analysis

Data are expressed as mean values ± SEM and were analyzed by the one-way ANOVA with Dunnett's post test was performed ($^*p < 0.05$ vs. control).

3. Results

3.1. Antagonistic effect of R1antTNF on wtTNF-α induced cytotoxicity and cytokine production

To confirm the potency of R1antTNF as an antagonist to the human TNFR1-specific bioactivity of wtTNF-α, we examined the inhibitory effect of R1antTNF on wtTNF-α induced cytotoxicity in HEp-2 cells. The cytotoxic activity of wtTNF-α was inhibited by R1antTNF in a dose-dependent manner. In particular, cell viability increased from 10% to 80% after treatment with R1antTNF at 3×10^5 ng/ml (Fig. 1A). R1antTNF alone showed almost no biolog-
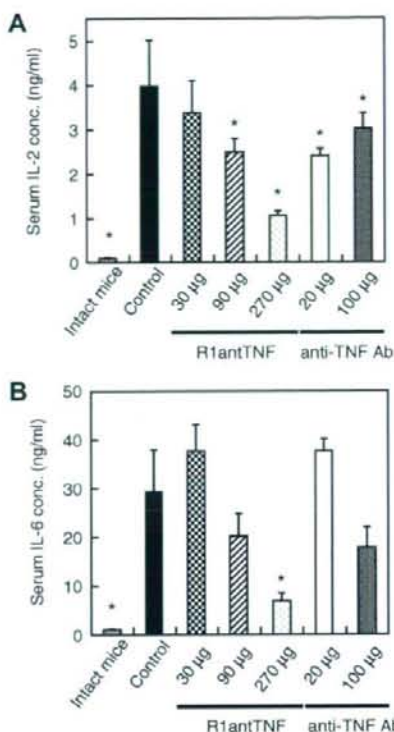
Fig. 3. Therapeutic effect of R1antTNF against ConA-induced hepatitis model. BALB/c mice (6-week-old female) were injected intravenously with ConA (0.4 mg/mouse). Anti-mouse TNF-α Ab or R1antTNF was injected 1 h after ConA injection. Blood samples were collected at 4 h after ConA injection. The serum IL-2 (A) and IL-6 (B) concentration was measured by ELISA ($n = 6$). Data represent the means ± SEM.

ver and serum ALT levels were decreased in TNFR1 knockout mice. In agreement with this, R1antTNF treatment clearly inhibited the elevation of ALT levels. However, remarkably when we used anti-TNF-α Ab as a reference for the efficacy of R1antTNF, we observed that administration of anti-TNF-α Ab increased ALT levels and even exacerbated liver failure, suggesting a paradoxical tissue protective effect of TNF-α. Similar observations were reported in a previous study, which reported that TNF-α induces the early-immediate inflammatory response through TNFR1 [27]. Additionally, it was reported that TNF-α plays an important role in the recovery from CCl₄-induced hepatitis through TNFR2 [28]. Thus, treatment with anti-TNF-α Ab may lead to adverse effects due to the lack of receptor-subtype specificity. These results indicate that R1antTNF may be more useful than anti-TNF-α Ab in treating TNFR1-dependent inflammatory diseases.

T-cell-mediated immune responses play a central role in hepatocellular injury induced by autoimmune hepatitis, viral infection, alcohol consumption, and hepatotoxins [29,30]. For example, CD4⁺ T-cells are the predominant population of T-cells infiltrating into the liver in human autoimmune liver disease [31]. Therefore, we examined the therapeutic effect of R1antTNF on ConA-induced hepatitis model. R1antTNF inhibited the elevation of IL-2 and IL-6, which is mainly secreted from activated T-cells and Kupffer cells respectively. The therapeutic effect of R1antTNF on ConA-induced hepatitis model is almost the same as that of anti-TNF-α Ab. Numerous reports have shown that treatment with LPS or TNF-α

in conjunction with ᴅ-galactosamine results in acute liver apoptosis and liver failure predominantly through TNFR1, resulting in activation of caspases and subsequent hepatocyte apoptosis [32,33]. However, studies by Kollias et al., and by Grell et al. have suggested that cell-associated TNF-α signaling through TNFR2 contributes to the development of rheumatoid arthritis and hepatocyte apoptosis [34–36]. Furthermore, investigators have argued that the liver injury from ConA treatment is not solely due to secreted TNF-α acting through TNFR1, but is also cell-associated TNF-α signaling through TNFR2 [35]. Thus, although the details of TNFR2-mediated signaling on hepatotoxicity are still unclear, it has been thought that the involvement of TNFR2 is different among hepatic models. Indeed, in our experiments, the treatment with anti-TNF-α Ab, which prevents TNF-α binding on both TNFR1 and TNFR2, exacerbated CCl₄-induced hepatitis model, but did not ConA-induced hepatitis model. Therefore, the fact that R1antTNF showed a substantial therapeutic effect in several hepatitis models is significant, and indicates the possibility that R1antTNF might be effective therapeutic agent for hepatitis caused by various factors.

One of the most common ways of enhancing the plasma half-lives of proteins is to conjugate them with polyethylene glycol (PEG) [37,38]. Because random introduction of PEG at the ε-amino groups of lysine residues usually lowers the bioactivity of proteins, application of PEGylation is generally limited to a small part of the protein. To overcome these problems of PEGylation, we recently developed a novel strategy for site-specific PEGylation via lysine-deficient mutant TNF-α, in which all of the lysine residues were replaced with other amino acids [19,20]. The lysine-deficient mutant TNF-α was site-specifically mono-PEGylated at its NH₂ terminus with PEG without loss of bioactivity. This site-specific mono-PEGylated mutant TNF-α showed increased in vivo therapeutic potency compared with the unmodified wtTNF-α and randomly mono-PEGylated wtTNF-α. R1antTNF was generated using a phage library based on this lysine-deficient mutant TNF-α and all of the lysine residues of R1antTNF were replaced with other amino acids [21]. We are currently attempting to construct mono-PEGylated R1ant-TNF. We anticipate that PEGylated R1antTNF will further enhance the anti-inflammatory activity for use in autoimmune disease models.

In conclusion, we have shown that R1antTNF is a useful TNF-α antagonist for treatment of hepatitis. Our results indicate that the therapeutic effect of R1antTNF can be equal or superior to that of anti-TNF-α Ab in treating TNFR1-dependent inflammatory diseases.

Acknowledgments

References

[1] Galun E, Axelrod JH. The role of cytokines in liver failure and regeneration: potential new molecular therapies. Biochim Biophys Acta 2002;1592:345–58.
[2] Vaquero J, Blei AT. Etiology and management of fulminant hepatic failure. Curr Gastroenterol Rep 2003;5:39–47.
[3] Lee WM. Acute liver failure in the United States. Semin Liver Dis 2003;23:217–26.
[4] Tracey KJ, Cerami A. Tumor necrosis factor: a pleiotropic cytokine and therapeutic target. Annu Rev Med 1994;45:491–503.
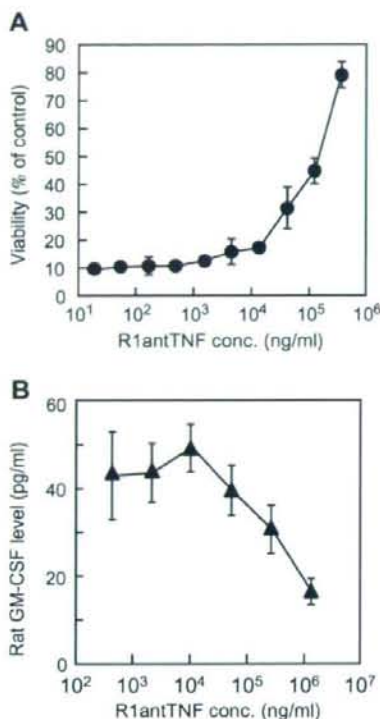
A

B

Fig. 1. Antagonistic activities of the R1antTNF. (A) Serial dilutions of R1antTNF were mixed with human wtTNF-α (20 ng/ml) and then applied to HEp-2 cells. After 18 h, the inhibitory effects of R1antTNF on the cytotoxicity of wtTNF-α were assessed by using the methylene blue assay. The absorbance of cells without wtTNF-α was plotted as 100 percent viability. (B) Serial dilutions of R1antTNF were mixed with human wtTNF-α (200 ng/ml) and applied to PC60-hTNFR1(+) cells (B). After 24 h, production of rat GM-CSF was quantified by ELISA. Rat GM-CSF was undetectable in the absence of wtTNF-α. The data represent the means ± SD (n = 3).

ical activity even when tested at 5×10^4 ng/ml (data not shown). We also confirmed the antagonistic effect of R1antTNF using another cell line. PC60-hTNFR1(+) cells, genetically engineered to express human TNFR1, were used to test the blocking activities of R1antTNF. R1antTNF efficiently inhibited wtTNF-α-mediated production of rat GM-CSF by PC60-hTNFR1(+) cells (Fig. 1B). The rat GM-CSF production mediated by wtTNF-α was not detected from PC60 cells, the parent cells of PC60-hTNFR1(+) cells. These results suggested that R1antTNF elicits an antagonistic effect against wtTNF-α through TNFR1.

3.2. Therapeutic effect of R1antTNF on hepatitis models

Firstly, we examined the therapeutic effect of R1antTNF in a CCl_4-induced hepatitis mouse model. CCl_4 is an industrial toxicant that is known to cause hepatic necrosis as well as free radical generation in kidney, heart, lung, testis, brain, and blood [23]. These reactive oxygen species can destroy cellular membranes, cellular proteins, and nucleic acids. The CCl_4-induced model has been extensively used as an experimental model of liver disease, such as hepatic cirrhosis and drug-induced hepatopathy. Injection of CCl_4-induced an accelerated serum ALT level, a well-characterized marker of liver damage. Treatment with R1antTNF, even at 30 μg/ mouse, strongly inhibited elevation in the serum level of ALT (Fig.
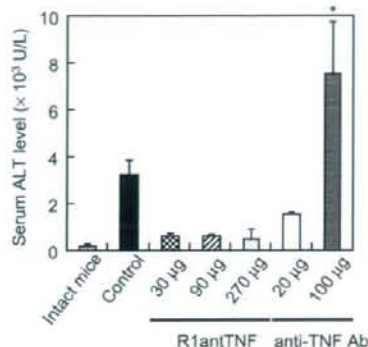

Fig. 2. Therapeutic effect of R1antTNF against the CCl_4-induced hepatitis model. BALB/c mice (6-week-old female) were intraperitoneally administered with CCl_4 at a dose of 0.1 ml/kg in corn oil (10 ml/kg). Intact animals received only corn oil. After 12 h, each mouse was given R1antTNF, anti-mouse TNF-α Ab, or PBS by intravenous injection. Blood samples were collected at 48 h after CCl_4 administration and serum ALT levels were then measured. Data represent the means ± SEM of three animals.

2). The serum level of ALT after treatment with R1antTNF at 30 μg/ mouse was lower than that observed after treatment with anti-TNF-α Ab at 20 μg/mouse. Interestingly, treatment with the anti-TNF Ab at 100 μg/mouse actually raised the serum ALT levels compared to control mice, and seemed to even aggravate the hepatic disorder. These results indicate that R1antTNF may be more useful than anti-TNF-α Ab in treating CCl_4-induced hepatitis.

ConA-induced hepatitis in mice is a well-characterized model of T-cell-mediated liver disease and has been extensively used as a prototype mimicking human T-cell-mediated liver disease [24]. It is associated with elevated serum ALT, IL-2 and IL-6, and hepatic lesions are characterized by a massive granulocyte and T-cell infiltration, followed by hepatocyte necrosis and apoptosis. Thus, to examine the inhibitory effect of R1antTNF on Con A-induced activation of immune cells, we determined the elevation of serum IL-2 and IL-6. Initially, we examined the serum level of the T-cell-derived cytokine IL-2. R1antTNF dose-dependently reduced the level of serum IL-2 compared to control mice (Fig. 3A). The IL-2 level of mice treated with R1antTNF at 90 μg/mouse was the same as that of mice treated with anti-TNF-α Ab at 100 μg/mouse. Treatment with R1antTNF at 270 μg/mouse resulted in an even greater reduction in the serum level of IL-2. Next, to determine the inhibitory effect of R1antTNF on macrophage activation, we examined the serum IL-6 level, which is predominantly produced by Kupffer cells [25,26]. As with IL-2, R1antTNF dose-dependently reduced the serum level of IL-6 compared to control mice (Fig. 3B). The therapeutic effect thought to result from that R1antTNF inhibited ConA-induced activation of T-cells and macrophages as effectively as anti-TNF-α Ab.

4. Discussion

Previously we generated R1antTNF, a novel TNFR1-selective antagonistic mutant of TNF-α. The antagonistic effect of R1antTNF was demonstrated in vivo using a D-(+)-galactosamine (GalN)/TNF-α-dependent acute inflammatory liver injury model [21]. In this study, to clarify the therapeutic potency of R1antTNF more precisely, we examined the therapeutic effect of R1antTNF in two hepatitis models and compared the therapeutic efficacy to that of anti-TNF-α Ab.

In CCl_4-induced hepatitis model, previous study indicated that inflammatory cell influx, induction of adherent molecules in the li-

[5] Aggarwal BB. Signalling pathways of the TNF superfamily: a double-edged sword. Nat Rev Immunol 2003;3:745–56.

[6] Muto Y, Nouri-Aria KT, Meager A, Alexander GJ, Eddleston AL, Williams R. Enhanced tumour necrosis factor and interleukin-1 in fulminant hepatic failure. Lancet 1988;2:72–4.

[7] Bird GL, Sheron N, Goka AK, Alexander GJ, Williams RS. Increased plasma tumor necrosis factor in severe alcoholic hepatitis. Ann Intern Med 1990;112:917–20.

[8] Gonzalez-Amaro R, Garcia-Monzon C, Garcia-Buey L, Moreno-Otero R, Alonso JL, Yague E, et al. Induction of tumor necrosis factor alpha production by human hepatocytes in chronic viral hepatitis. J Exp Med 1994;179:841–8.

[9] Bradham CA, Plumpe J, Manns MP, Brenner DA, Trautwein C. Mechanisms of hepatic toxicity. I. TNF-induced liver injury. Am J Physiol 1998;275:G387–92.

[10] McClain CJ, Song Z, Barve SS, Hill DB, Deaciuc I. Recent advances in alcoholic liver disease. IV. Dysregulated cytokine metabolism in alcoholic liver disease. Am J Physiol Gastrointest Liver Physiol 2004;287:G497–502.

[11] Menon KV, Stadheim L, Kamath PS, Wiesner RH, Gores GJ, Peine CJ, et al. A pilot study of the safety and tolerability of etanercept in patients with alcoholic hepatitis. Am J Gastroenterol 2004;99:255–60.

[12] Carroll MB, Bond MI. Use of tumor necrosis factor-alpha inhibitors in patients with chronic hepatitis B infection. Semin Arthritis Rheum 2008, in press.

[13] Keane J, Gershon S, Wise RP, Mirabile-Levens E, Kasznica J, Schwieterman WD, et al. Tuberculosis associated with infliximab, a tumor necrosis factor alpha-neutralizing agent. N Engl J Med 2001;345:1098–104.

[14] Shakoor N, Michalska M, Harris CA, Block JA. Drug-induced systemic lupus erythematosus associated with etanercept therapy. Lancet 2002;359:579–80.

[15] Aggarwal BB, Eessalu TE, Hass PE. Characterization of receptors for human tumour necrosis factor and their regulation by gamma-interferon. Nature 1985;318:665–7.

[16] Wajant H, Pfizenmaier K, Scheurich P. Tumor necrosis factor signaling. Cell Death Differ 2003;10:45–65.

[17] MacEwan DJ. TNF receptor subtype signalling: differences and cellular consequences. Cell Signal 2002;14:477–92.

[18] Bradley J. TNF-mediated inflammatory disease. J Pathol 2008;214:149–60.

[19] Yamamoto Y, Tsutsumi Y, Yoshioka Y, Nishibata T, Kobayashi K, Okamoto T, et al. Site-specific PEGylation of a lysine-deficient TNF-alpha with full bioactivity. Nat Biotechnol 2003;21:546–52.

[20] Shibata H, Yoshioka Y, Ikemizu S, Kobayashi K, Yamamoto Y, Mukai Y, et al. Functionalization of tumor necrosis factor-alpha using phage display technique and PEGylation improves its antitumor therapeutic window. Clin Cancer Res 2004;10:8293–300.

[21] Shibata H, Yoshioka Y, Ohkawa A, Minowa K, Mukai Y, Abe Y, et al. Creation and X-ray structure analysis of the tumor necrosis factor receptor-1-selective mutant of a tumor necrosis factor-alpha antagonist. J Biol Chem 2008;283:998–1007.

[22] Vandenabeele P, Declercq W, Vanhaesebroeck B, Grooten J, Fiers W. Both TNF receptors are required for TNF-mediated induction of apoptosis in PC60 cells. J Immunol 1995;154:2904–13.

[23] Recknagel RO, Glende Jr EA, Dolak JA, Waller RL. Mechanisms of carbon tetrachloride toxicity. Pharmacol Ther 1989;43:139–54.

[24] Tiegs G, Hentschel J, Wendel A. A T cell-dependent experimental liver injury in mice inducible by concanavalin A. J Clin Invest 1992;90:196–203.

[25] Mizuhara H, O'Neill E, Seki N, Ogawa T, Kusunoki C, Otsuka K, et al. T cell activation-associated hepatic injury: mediation by tumor necrosis factors and protection by interleukin 6. J Exp Med 1994;179:1529–37.

[26] Wolf AM, Wolf D, Rumpold H, Ludwiczek S, Enrich B, Gastl G, et al. The kinase inhibitor imatinib mesylate inhibits TNF-{alpha} production in vitro and prevents TNF-dependent acute hepatic inflammation. Proc Natl Acad Sci USA 2005;102:13622–7.

[27] Bruccoleri A, Gallucci R, Germolec DR, Blackshear P, Simeonova P, Thurman RG. et al. Induction of early-immediate genes by tumor necrosis factor alpha contribute to liver repair following chemical-induced hepatotoxicity. Hepatology 1997;25:133–41.

[28] Yamada Y, Fausto N. Deficient liver regeneration after carbon tetrachloride injury in mice lacking type 1 but not type 2 tumor necrosis factor receptor. Am J Pathol 1998;152:1577–89.

[29] Kita H, Mackay IR, Van De Water J, Gershwin ME. The lymphoid liver: considerations on pathways to autoimmune injury. Gastroenterology 2001;120:1485–501.

[30] Heneghan MA, McFarlane IG. Current and novel immunosuppressive therapy for autoimmune hepatitis. Hepatology 2002;35:7–13.

[31] Lohr HF, Schlaak JF, Lohse AW, Bocher WO, Arenz M, Gerken G, et al. Autoreactive CD4+ LKM-specific and anticlonotypic T-cell responses in LKM-1 antibody-positive autoimmune hepatitis. Hepatology 1996;24:1416–21.

[32] Rothe J, Lesslauer W, Lotscher H, Lang Y, Koebel P, Kontgen F, et al. Mice lacking the tumour necrosis factor receptor 1 are resistant to TNF-mediated toxicity but highly susceptible to infection by Listeria monocytogenes. Nature 1993;364:798–802.

[33] Nowak M, Gaines GC, Rosenberg J, Minter R, Bahjat FR, Rectenwald J, et al. LPS-induced liver injury in D-galactosamine-sensitized mice requires secreted TNF-alpha and the TNF-p55 receptor. Am J Physiol Regul Integr Comp Physiol 2000;278:R1202–9.

[34] Grell M, Douni E, Wajant H, Lohden M, Clauss M, Maxeiner B, et al. The transmembrane form of tumor necrosis factor is the prime activating ligand of the 80 kDa tumor necrosis factor receptor. Cell 1995;83:793–802.

[35] Kusters S, Tiegs G, Alexopoulou L, Pasparakis M, Douni E, Kunstle G, et al. In vivo evidence for a functional role of both tumor necrosis factor (TNF) receptors and transmembrane TNF in experimental hepatitis. Eur J Immunol 1997;27:2870–5.

[36] Alexopoulou L, Pasparakis M, Kollias G. A murine transmembrane tumor necrosis factor (TNF) transgene induces arthritis by cooperative p55/p75 TNF receptor signaling. Eur J Immunol 1997;27:2588–92.

[37] Yoshioka Y, Tsutsumi Y, Nakagawa S, Mayumi T. Recent progress on tumor missile therapy and tumor vascular targeting therapy as a new approach. Curr Vasc Pharmacol 2004;2:259–70.

[38] Mukai Y, Yoshioka Y, Tsutsumi Y. Phage display and PEGylation of therapeutic proteins. Comb Chem High Throughput Screen 2005;8:145–52.

Research paper

Simple and highly sensitive assay system for TNFR2-mediated soluble- and transmembrane-TNF activity

Yasuhiro Abe [a,b], Tomoaki Yoshikawa [a,c], Haruhiko Kamada [a,d], Hiroko Shibata [a,e], Tetsuya Nomura [a,b], Kyoko Minowa [a,f], Hiroyuki Kayamuro [a,b], Kazufumi Katayama [g], Hiroyuki Miyoshi [h], Yohei Mukai [a,b], Yasuo Yoshioka [a,c], Shinsaku Nakagawa [b], Shin-ichi Tsunoda [a,d,*], Yasuo Tsutsumi [a,b,d]

[a] Laboratory of Pharmaceutical Proteomics, National Institute of Biomedical Innovation, 7-6-8 Saito-Asagi, Ibaraki, Osaka 567-0085, Japan
[b] Graduate School of Pharmaceutical Sciences, Osaka University, 1-6 Yamadaoka, Suita, Osaka 565-0871, Japan
[c] The Center for Advanced Research and Education in Drug Discovery and Development, Osaka University, 1-6 Yamadaoka, Suita, Osaka 565-0871, Japan
[d] The Center for Advanced Medical Engineering and Informatics, Osaka University, 1-6 Yamadaoka, Suita, Osaka 565-0871, Japan
[e] Division of Drugs, National Institute of Health Science, 1-18-1 Kamiyoga, Setagaya-ku, Tokyo 158-8501, Japan
[f] Graduate School of Pharmaceutical Sciences, Kyoto Pharmaceutical University, Misasagi-Nakauchicho 5, Yamashina-ku, Kyoto 607-8414, Japan
[g] Allergy & Immunology Project, Tokyo Metropolitan Institute of Medical Science, 3-18-22, Honkomagome, Bunkyo-ku, Tokyo 113-8613, Japan
[h] Subteam for Manipulation of Cell Fate, BioResource Center, RIKEN, 3-1-1 Koyadai, Tsukuba, Ibaraki 305-0074, Japan

ARTICLE INFO

ABSTRACT

Drugs that target tumor necrosis factor-α (TNF) are particularly important in the treatment of severe inflammatory progression in rheumatoid arthritis, Crohn's disease and psoriasis. Despite the central role of the TNF/TNF receptor (TNFR) in various disease states, there is a paucity of information concerning TNFR2 signaling. In this study, we have developed a simple and highly sensitive cell-death based assay system for analyzing TNFR2-mediated bioactivity that can be used to screen for TNFR2-selective drugs. Using a lentiviral vector, a chimeric receptor was engineered from the extracellular and transmembrane domain of human TNFR2 and the intracellular domain of mouse Fas and the recombinant protein was then expressed in TNFR1^{−/−}R2^{−/−} mouse preadipocytes. Our results demonstrate that this chimeric receptor is capable of inducing apoptosis by transmembrane- as well as soluble-TNF stimuli. Moreover, we found that our bioassay based on cell death phenotype had an approximately 80-fold higher sensitivity over existing bioassays. We believe our assay system will be an invaluable research tool for studying TNFR2 and for screening TNFR2-targeted drugs.

© 2008 Elsevier B.V. All rights reserved.

1. Introduction

Tumor necrosis factor-α (TNF) is a pleiotropic cytokine that regulates various biological processes such as host defense, inflammation, autoimmunity, apoptosis and tumor cell death through the TNF-receptor 1 (TNFR1) and receptor 2 (TNFR2) (Wajant et al., 2003). TNF/TNFR interaction is considered to be an attractive target for the treatment of refractory diseases, including autoimmune disease and malignant tumors (Aggarwal, 2003; Szlosarek and Balkwill, 2003). In rheumatoid arthritis, for example, biological anti-TNF agents, such as Infliximab and Adalimumab, rapidly reduce signs and symptoms of joint inflammation (Feldmann and Maini, 2003). However, anti-TNF drugs used to treat inflammatory disorders have been reported to increase the risk of infection, in accordance with animal studies (Brown et al., 2002; Nathan et al., 2006).

A thorough understanding of the biology of the TNF/TNFR system is a prerequisite to the safe and effective development of anti-TNF therapeutics. In particular, several factors and mechanisms hypothesized to be involved in the side effects elicited by anti-TNF drugs need to be tested (Curtis et al., 2007; Jacobs et al., 2007; Schneeweiss et al., 2007). These include the differential power of the drugs to neutralize TNF bioavailability and the differential inhibition of TNF signaling events. Despite extensive studies on the molecular biology of TNF/TNFR1 signaling (Micheau and Tschopp, 2003) the functions of TNFR2 are poorly understood. There is an increasing need for a comprehensive understanding of TNF/TNFR2 biology, particularly in terms of the development of TNFR-selective drugs.

In this context, we have used a novel phage-display based screening system (Yamamoto et al., 2003; Shibata et al., 2004, 2008) to develop structural mutants of TNF to help clarify the biology of TNF/TNFR2 interactions. These TNF variants, which exert TNFR2-mediated agonistic or antagonistic activity, might be extremely valuable for elucidating structure-activity relationships between TNF and TNFR2. So far, in order to evaluate the bioactivity of TNF through TNFR2, many researchers have used the TNFR2 over-expressing cell lines (Heller et al., 1992; Weiss et al., 1998), such as rat/mouse T hybridomas transfected with human TNFR2 (PC60-hR2) (Vandenabeele et al., 1992). The PC60-hR2 assay is based on granulocyte macrophage colony-stimulating factor (GM-CSF) secretion mediated by TNF/TNFR2 stimuli. The GM-CSF secretion level is quantified by proliferation of GM-CSF-dependent cell lines or by ELISA. However, this two-step assay system is complicated and the screening process is highly laborious. Thus, there are increasing demands for the development of a simple, highly sensitive screening system that is TNFR2-selective.

In the present study, we developed a simple but highly sensitive cell death-based assay system for evaluating TNFR2-mediated activity. We constructed a lentiviral vector expressing a chimeric receptor derived from the extracellular (EC) and transmembrane (TM) domain of human TNFR2 (hTNFR2) and the intracellular (IC) domain of mouse Fas (mFas). Additionally, to eliminate the influence of the endogenous TNFR1, the chimeric receptor was expressed on TNFR1$^{-/-}$R2$^{-/-}$ preadipocytes (Xu et al., 1999). We found that hTNFR2/mFas-expressing preadipocyte (hTNFR2/mFas-PA) showed about 80-times higher sensitivity after treatment with soluble-TNF and over the conventional method. Furthermore, hTNFR2/mFas-PA could detect not only transmembrane TNF- (tmTNF) but also soluble TNF-activity. The technology described herein will be highly useful both as an assay system for various TNF variants via TNFR2 and also as a cell-based drug discovery system for TNFR2 agonists/antagonists.

2. Materials and methods

2.1. Cell culture

TNFR1$^{-/-}$R2$^{-/-}$, TNFR1$^{-/-}$, and wild-type (wt) preadipocytes established from day 16–17 mouse embryos were generously provided by Dr. Hotamisligil (Harvard School of Public Health, Boston MA). Preadipocytes, 293T cells and HeLaP4 cells were cultured in Dulbecco's modified Eagle's medium (DMEM; Sigma-Aldrich, Inc., Tokyo, Japan) with 10% bovine fetal serum (FBS) and 1% antibiotic cocktail (penicillin 10,000 u/ml, streptomycin 10 mg/ml, and amphotericin B 25 μg/ml; Nacalai Tesque, Kyoto, Japan). The rat/mouse T hybridomas PC60-hR2 cells (hTNFR2 transfected PC60 cells) were generously provided by Dr. Vandenabeele (University of Gent, Belgium) and cultured in RPMI 1640 (Sigma-Aldrich, Inc.) with 10% FBS, 1 mM sodium pyrubate, 5×10^{-5} M 2-ME, 3 μg/ml puromycin (Wako Pure Chemical Industries, Osaka, Japan), and 1% antibiotic cocktail. TNFR1$^{-/-}$R2$^{-/-}$ mouse macrophages were generously provided by Dr. Aggarwal (University of Texas MD Anderson Cancer Center, Houston, TX), and cultured in RPMI 1640 with 10% FBS and 1% antibiotic cocktail.

2.2. Construction of self-inactivating (SIN) lentiviral vector

Vectors were constructed using standard cloning procedures. A DNA fragment encoding the EC and TM parts of hTNFR2 was amplified by polymerase chain reaction (PCR) from human peripheral blood lymphocyte cDNA with the following primer pairs: forward primer (5'-GAT TAC GCC AAG CTT GTC GAC CAC CAT GGC GCC CGT CGC CGT CTG GGC CGC GCT GGC CGT CGG ACT GGA G-3') containing a SalI site at the 5'-end and a reverse primer (5'-CAC CTT GGC TTC TCT CTG CTT TCG AAG GGG CTT CTT TTT CAC CTG GGT CA-3') containing a Csp45I site. The resulting amplified fragment was subcloned into pCR-Blunt II-TOPO (Invitrogen Corp., Carlsbad, CA) to generate pCR-Blunt-hTNFR2. A fragment encoding the IC domain of mFas was amplified by PCR from mouse spleen cDNA with the following primer pair: forward primer (5'-AAT TCC ACT TGT ATT TAT ACT TCG AAA GTA CCG GAA AAG A-3') containing a Csp45I site and a reverse primer (5'-GTC ATC CTT GTA GTC TGC GGC CGC TCA CTC CAG ACA TTG TCC TTC ATT TTC ATT TCC A-3') containing a NotI site at the 5'-end. The mFas DNA fragment was subcloned into pCR-Blunt-hTNFR2 between the Csp45I and NotI sites to combine the EC and TM domains of hTNFR2 to the IC domains of mFas, generating pCR-Blunt-hTNFR2/mFas (Fig. 1A). Then the hTNFR2/mFas DNA fragment was cloned between the XhoI and NotI sites of SIN lentiviral vector construct, which contains the blasticidin (Bsd) resistance gene, generating CSII-CMV-hTNFR2/mFas-IRES2-Bsd (Fig. 1B). For construct tmTNF, a DNA fragment encoding non-cleavable human tmTNF h(tmTNFΔ1-12), generated by deleting amino acids 1–12 in the N-terminal part of hTNF, was amplified by PCR from hTNF cDNA with following primer pair: forward primer (5'-AGT GAT CGG CCC CCA GAG GGA AGC TTA GAT CTC TCT CTA ATC AGC CCT CTG GCC CAG GCA GTA GCC CAT GTT GTA GCA AAC CCT CAA G-3') and reverse primer (5'-GGT TGG ATG TTC GTC CTC CGC GGC CGC CTA ACT AGT TCA CAG GGC AAT GAT CCC AAA GTA GAC CTG-3') and cloned into the pY03' vector. Then tmTNFΔ1–12 DNA fragment was cloned between the SalI and XhoI sites of the SIN vector construct, generating CSII-EF-tmTNF-IRES-GFP.

2.3. Preparation of lentiviral vectors

The method used to prepare the lentiviral vector has been described previously (Miyoshi et al., 1999; Katayama et al.,
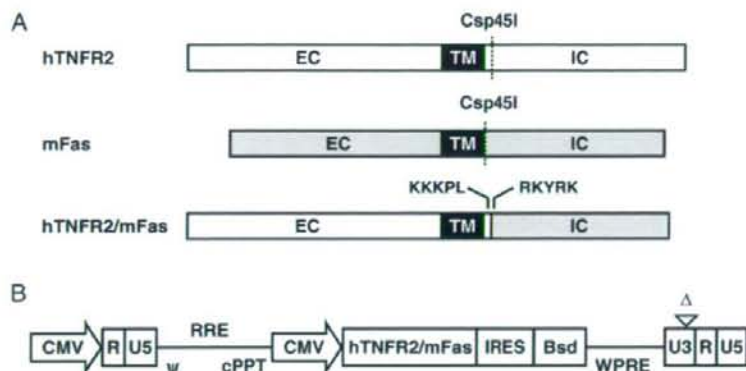
Fig. 1. Construction of hTNFR2/mFas chimeric receptor gene and vector. (A) The cDNA structures of hTNFR2, mFas and fusion genes (hTNFR2/mFas) are shown. EC: extracellular domain, TM: transmembrane domain, IC: Intracellular domain. (B) Schematic representation of self-inactivating (SIN) LV plasmid (CSII-CMV-hTNFR2/mFas-IRES-Bsd). CMV, cytomegalovirus promoter; ψ: packaging signal; RRE, rev responsive element; cPPT, central polypurine tract; IRES, Encephalomyocarditis virus internal ribosomal entry site; Bsd, Blasticidin; WPRE, woodchuck hepatitis virus posttranscriptional regulatory element. Δ: deleting 133 bp in the U3 region of the 3' long terminal repeat.

2004). In brief, 293T cells were transfected by the calcium phosphate method with three plasmids: packaging construct (pCAG-HIVgp), VSV-G and Rev expressing construct (pCMV-VSV-G-RSV-Rev) and SIN vector construct (CSII-CMV-TNFR2/Fas-IRES2-Bsd or CSII-EF-tmTNF-IRES-GFP). Two days after transfection, the conditioned medium was collected and the virus was concentrated by ultracentrifugation at 50,000 × g for 2 h at 20 °C. The pelleted virus was resuspended in Hanks' balanced salt solution (GIBCO BRL, Paisley, UK). Vector titers were determined by measuring the infectivity of HeLaP4 cells with serial dilutions of vector stocks using flow cytometric analysis (FCM) for hTNFR2/mFas- or GFP-positive cells.

2.4. Preparation of hTNFR2/mFas- or tmTNF-expressing cell culture

To prepare the hTNFR2/mFas- or tmTNF-expressing cell culture, TNFR1$^{-/-}$R2$^{-/-}$ preadipocytes or TNFR1$^{-/-}$R2$^{-/-}$ macrophages were infected with each lentiviral vector at a multiplicity of infection (MOI) of 100. Stable hTNFR2/mFas-transfectants were selected for growth in culture medium containing 8 μg/ml Bsd (Invitrogen Corp.) for 1 week. Expression of hTNFR2/mFas chimeric receptor on Bsd-resistant cells was detected by staining with biotinylated anti-hTNFR2 antibody (BD Biosciences, Franklin Lakes, NJ) at 0.5 μg/5×10^5 cells for 30 min at 4 °C. Subsequently, the cells were washed and stained with streptavidin-PE conjugate (BD Biosciences). The cell suspension was centrifuged at 800 × g, washed with PBS, centrifuged again, and then re-suspended in 500 μl of 0.4% paraformaldehyde. Fluorescence was analyzed on a FACS Vantage flow cytometer, and data were analyzed using CellQuest software (both BD Biosciences). The hTNFR2/mFas-positive cell cultures were used in subsequent experiments as hTNFR2/mFas-PA cells. For preparation of tmTNF-expressing TNFR1$^{-/-}$R2$^{-/-}$ macrophages (tmTNF-Mφ), IRES-driven GFP positive cells were sorted by FACSAria (BD Biosciences).

2.5. Cytotoxicity assays

Cells were seeded on 96-well micro titer plates at a density of 1.5×10^4 cells/well in culture medium. Serial dilutions of mouse or human TNF (mTNF or hTNF; Peprotech, Rocky Hill, NJ), anti-mFas antibody (clone Jo2; BD Biosciences), or paraformaldehyde-fixed tmTNF-Mφ were prepared with DMEM containing 1 μg/ml cycloheximide, and added to each well. After 48 h incubation, the cell viability was measured by WST-8 assay kit (Nacalai Tesque) according to the manufacturer's instructions. The assay is based on cleavage of the tetrazolium salt WST-8 to formazan by cellular mitochondrial dehydrogenase.

2.6. Induction of GM-CSF secretion on PC60-hR2

5×10^4 of PC60-hR2 cells were seeded on a 96 well plate and then exposed to a serial dilution of hTNF in the presence of IL-1β (2 ng/ml). After 24 h incubation, hTNFR2-mediated GM-CSF secretion on PC60-hR2 cells was quantified by ELISA kit according to the manufacturer's protocol (R&D Systems, Minneapolis, MN).

2.7. Immunoprecipitation and western blotting

For immunoprecipitation we used FLAG-TNF (a FLAG-tag fusion protein of hTNF), which was generated in E. coli and purified in our laboratory. The protocol for the expression and purification of recombinant proteins has been described previously (Yamamoto et al., 2003). 1×10^7 hTNFR2/mFas-PA cells were treated with or without 100 ng/ml of FLAG-TNF for 30 min at 37 °C. Cells were then harvested and lysed in 1 ml of lysis buffer (50 mM Tris HCl, pH 7.4, 150 mM NaCl, 1% Triton X-100, 1 mM EDTA and protease inhibitor cocktail; Sigma-Aldrich Inc.) and gently rocked at 4 °C for 30 min. Cell debris was removed by centrifugation at 10,000 ×g for 30 min. The resulting supernatant was immunoprecipitated with anti-FLAG-M2 affinity beads (Sigma, St.Louis, MO) for 4 h at 4 °C. Immune complexes bound to the beads were washed three

times with 500 µl of lysis buffer and eluted with 3×FLAG peptide at a concentration of 150 ng/ml. Collected proteins were resolved on 10–20% SDS-PAGE gels and transferred to polyvinylidene fluoride membranes (Millipore Corp., Billerica, MA) by electroblotting. Western blot analyses were performed with biotinylated anti-hTNFR2 antibody (R&D systems) or anti-FADD (Fas-associated death domain protein) antibody (H-181; Santa Cruz Biotechnology Inc., Santa Cruz, CA). Bound primary antibodies were visualized with horseradish peroxidase-conjugated streptavidin or goat–anti-rabbit-IgG (Jackson Immunoresearch Lab., West Grove, PA) respectively, and ECL plus western blotting detection reagents (GE Healthcare, Buckinghamshire, UK). A LAS 3000 image analyzer (Fujifilm, Tokyo, Japan) was used for the observation of chemiluminescence.

3. Results

3.1. Fas- but not TNFR-mediates induction of cell-death in TNFR1$^{-/-}$R2$^{-/-}$ preadipocytes

Initially, we established a cell line that could be used to evaluate TNFR2-specific bioactivity by means of the chimeric receptor (hTNFR2/mFas) strategy. The parental cell line must
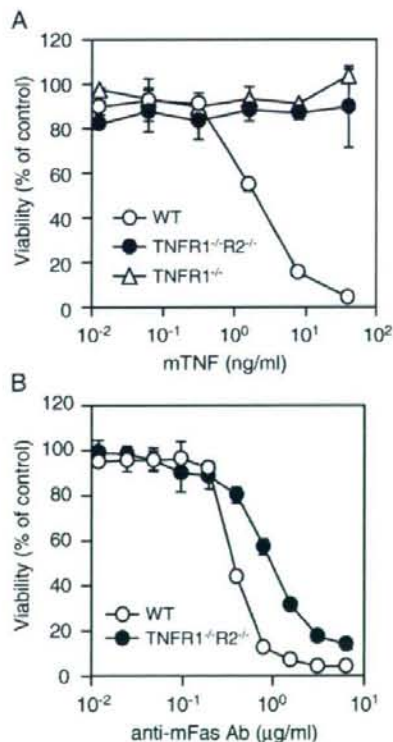

Fig. 2. Fas, but not TNFR2, induced cell death in preadipocytes. WT, TNFR1$^{-/-}$R2$^{-/-}$ and TNFR1$^{-/-}$ cells were treated with serial dilutions of (A) mTNF or (B) anti-mFas Ab. Cell viability was determined using the WST-8 Assay. Each data point represents the mean±SD of triplicate wells.
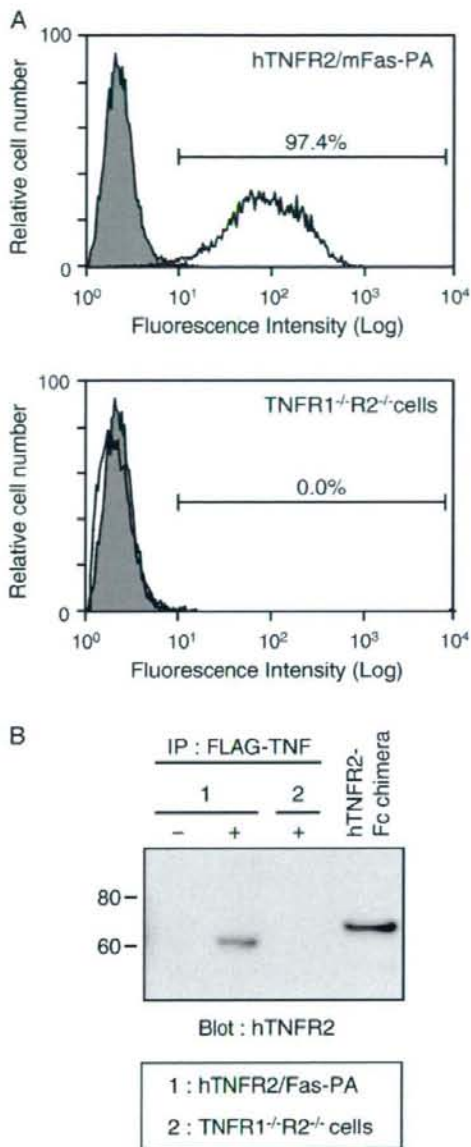

Fig. 3. Expression of hTNF2/mFas chimeric receptor on transfectants. (A) Expression of the chimeric receptor on hTNFR2/mFas-PA (upper panel) or parental TNFR1$^{-/-}$R2$^{-/-}$ cells (lower panel) was analyzed by flow cytometry using hTNFR2-specific antibody (open histograms) or isotype control antibody (shaded histograms). (B) hTNFR2/mFas-PA or TNFR1$^{-/-}$R2$^{-/-}$ cells were treated (+) with FLAG-TNF; (−) denotes untreated control cells. Immunoprecipitation was performed with anti-FLAG antibody M2-conjugated beads. After extensive washing, the immunocomplexes were eluted with 3×FLAG peptide. Eluted proteins were resolved on 10–20% SDS-PAGE gels and the presence of hTNFR2/mFas in the complex was detected by western blot using anti-hTNFR2 antibody.
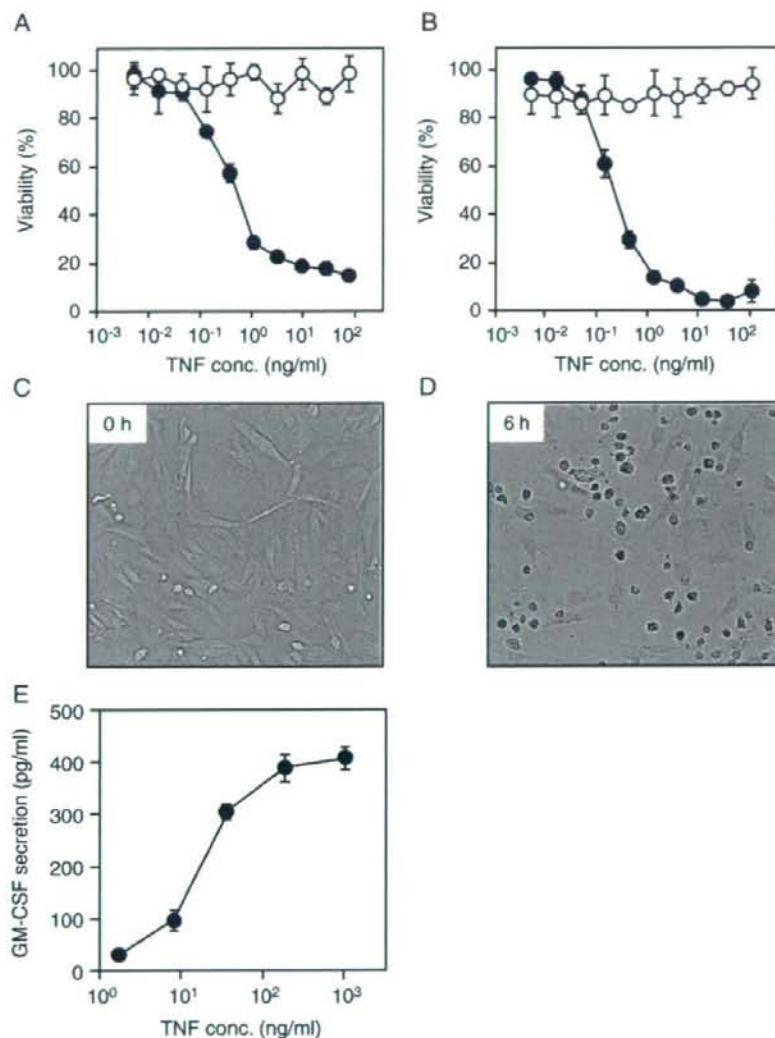
Fig. 4. Induction of strong cell death on hTNFR2/mFas-PA by soluble hTNF. hTNFR2/mFas-PA (●) and parental TNFR1$^{-/-}$R2$^{-/-}$ (○) cells were treated with serial dilutions of hTNF in the presence of cycloheximide (1 μg/ml). After (A) 24 h and (B) 48 h, the cell viability was measured using the WST-8 Assay. Data from the WST-8 assay represents the mean and SDs of triplicate assays. Similar results were obtained in three independent experiments. (C) Untreated or (D) hTNF-treated (10 ng/ml) hTNFR2/mFas-PA cells were incubated for 6 h, and were assessed by light microscopy. (E) PC60-hR2 cells were incubated in the presence of a serial dilution of hTNF and IL-1β (2 ng/ml). After 24 h, induction of GM-CSF was determined by ELISA. Each data point represents the mean±SD of triplicate measurements.

possess both Fas-sensitivity and TNF-resistance. Thus, we selected TNFR1$^{-/-}$R2$^{-/-}$ preadipocytes as the parental cell line and then examined the susceptibility of this cell line against TNFR1- and Fas-induced cell death. TNFR1$^{-/-}$R2$^{-/-}$ preadipocytes were resistant to TNF-induced cell death, while WT preadipocytes, which co-express both TNFR1 and TNFR2, were killed by mTNF-treatment in a dose-dependent manner (Fig. 2A). TNFR1$^{-/-}$ preadipocytes were also resistant

to TNF-induced cell death. Thus, TNF-mediated cell death is presumably due to TNFR1-stimuli in accordance with previous reports (Vandenabeele et al., 1995; Ashkenazi and Dixit, 1998; Devin et al., 2000). Anti-Fas antibody treatment induced cell death for both WT, R1$^{-/-}$ and TNFR1$^{-/-}$R2$^{-/-}$ preadipocytes (Fig. 2B). Based on these results, we therefore selected TNFR1$^{-/-}$R2$^{-/-}$ preadipocytes for constructing an hTNFR2/mFas-expressing cell line.

3.2. hTNFR2-expression analysis of LV-hTNFR2/mFas-Bsd infected Bsd-resistant cells

Using the LV technique followed by Bsd selection, we established transfectants that stably expressed hTNFR2/mFas chimeric receptor in which the EC and TM portion of hTNFR2 (amino acids 1–292) was fused to the IC region of mFas (amino acids 187–328) (Figs. 1A and B). FCM analysis revealed that almost 95% of Bsd-resistant cells expressed the EC domain of hTNFR2 (Fig. 3A). To determine whether hTNFR2/mFas retained binding activity against hTNF, we next performed immunoprecipitation and western blot analysis (Fig. 3B). These analyses showed that FLAG-TNFs were immunoprecipitated and eluted with hTNFR2/mFas from LV-transfected and Bsd-resistant cells, but not from parental TNFR1$^{-/-}$R2$^{-/-}$ preadipocytes and untreated cells. Thus, we succeeded in constructing hTNFR2/mFas expressing TNFR1$^{-/-}$R2$^{-/-}$ preadipocytes that retained the ability to bind hTNF.

3.3. Induction of apoptosis on hTNFR2/mFas-PA

To examine whether the death signal could be transduced by stimulating the chimeric receptors, we evaluated the cell viability of soluble hTNF-treated hTNFR2/mFas-PA. As anticipated, addition of hTNF to hTNFR2/mFas-PA induced a strong cytotoxic effect 24 and 48 h later, whereas no cell death was detected using parental TNFR1$^{-/-}$R2$^{-/-}$ preadipocytes (Figs. 4A and B). After 48 h, more than 90% of hTNFR2/mFas-PA cells were killed by hTNF at a concentration of 4 ng/ml, resulting in a median effective concentration (EC50) of 250 pg/ml. The images in Figs. 4C and D show that hTNFR2/mFas-PA cells underwent clear morphological changes, indicating apoptosis by hTNF stimuli. Additionally, PC60-hR2 cells were tested for hTNFR2-mediated GM-CSF secretion (Fig. 4E). The concentration required to induce 50% of maximal secretion of GM-CSF obtained with hTNF (EC50) was approximately 20 ng/ml. Importantly, our bioassay based on cell death phenotype displayed a ~80-fold higher level of sensitivity over conventional methodol-

IP : FLAG-TNF

Blot : FADD

Fig. 6. Recruitment of FADD to the hTNFR2/mFas chimeric receptor in response to hTNF. hTNFR2/mFas-PA or TNFR1$^{-/-}$R2$^{-/-}$ cells were treated (+) with FLAG-TNF; (−) denotes untreated cells. Immunoprecipitation was performed with anti-FLAG antibody M2-conjugated beads. After extensive washing, immunocomplexes were eluted with 3×FLAG peptide. The eluted proteins were resolved on 10–20% SDS-PAGE gels and the presence of hTNFR2/mFas in the complex was detected by western blot using anti-FADD Antibody.

ogies. Moreover, tmTNF (Fig. 5) and anti-TNFR2 agonistic antibody (data not shown) induced hTNFR2/mFas-PA cell death.

3.4. Recruitment of FADD to the hTNFR2/mFas chimeric receptor

Recent studies indicate that some TNFR family members, including Fas, self-associate as trimers prior to ligand binding. Activation of the pre-associated receptors is triggered by ligand-induced rearrangement of the assembled trimers (Algeciras-Schimnich et al., 2002). We speculated that the first reaction after ligand-induced oligomerization of hTNFR2/mFas might be the recruitment of FADD, leading to caspase-8 activation. To investigate the composition of the ligand-hTNFR2/mFas signaling complex, we treated hTNFR2/mFas-PA cells with FLAG-tagged hTNF and affinity purified the receptor complex using anti-FLAG antibody-conjugated beads, followed by western blot analysis with antibody against FADD. As expected, FADD was immunoprecipitated with hTNFR2/mFas on hTNF-treated hTNFR2/mFas-PA (Fig. 6). In similar experiments, we could not detect TRADD, which is recruited to TNFR1 in a ligand-dependent process (data not shown). It has been reported that, in contrast to TNFR1, Fas does not interact with TRADD but directly recruits FADD, leading to efficient cell death (Stanger et al., 1995; Dempsey et al., 2003). Because hTNFR2/mFas interacts with FADD, our hTNFR2/mFas-PA cell-based assay system will be useful for evaluating hTNF activity specifically via hTNFR2.

4. Discussion

Here, we developed a hTNFR2/mFas-PA cell-based assay system in order to investigate hTNF activity through hTNFR2. The assay is simple to perform and can detect hTNF-mediated hTNFR2 activity with high sensitivity. Because the hTNFR2/
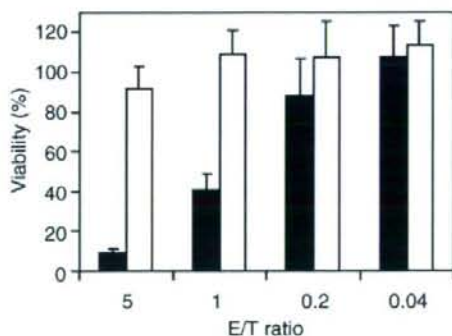

Fig. 5. hTNFR2/mFas-PA cells could be induced cell death by tmTNF. hTNFR2/mFas-PA cells were co-incubated with paraformaldehyde-fixed tmTNF-Mφ (filled bars) or TNFR1$^{-/-}$R2$^{-/-}$ Mφ (open bars) at an effector/target (E/T) ratio of 5:1, 1:1, 0.2:1 and 0.4:1 in the presence of cycloheximide (1 μg/ml). After 48 h, cell viability was measured by WST-8 Assay. Each data point represents the mean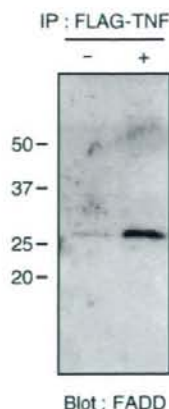±SD of triplicate measurements.